energy&fuels

Article

pubs.acs.org/EF

Effect of the Temperature on the Non-Newtonian Behavior of Heavy Oils

Enrique Soto-Castruita, Patsy V. Ramírez-González, Ulises Martínez-Cortés, and Sergio E. Quiñones-Cisneros*

Instituto de Investigaciones en Materiales, Universidad Nacional Autónoma de México, 04510 Mexico City, Mexico

ABSTRACT: The rheological behavior of heavy oils is critical for oil exploitation in different stages, such as extraction, transportation, and refining; during this process, the oil undergoes temperature changes that directly affect the viscosity. For light oils, the viscosity decreases around 1 order of magnitude when the temperature increases 100 K, whereas for heavy oils, this change could be of more than 3 orders of magnitude for the same temperature increment. Furthermore, the heavy oils exhibit a viscoelastic behavior, usually characterized by a viscosity reduction with the increment in the shear rate, the presence of elasticity, and time-dependent rheological behavior. As the temperature increases, the oils acquire a Newtonian behavior. This change is illustrated with the rheological characterization of five heavy oils with an American Petroleum Institute (API) gravity around 12°, different compositions, and zero-shear viscosity that varies up to 2 orders of magnitude among oils. The measurements were carried out in a controlled stress rheometer using a 40 mm parallel plate geometry with a gap of 1 mm. The fluids were tested in rotational and oscillatory modes at temperatures from 5 to 100 °C. In the oscillatory experiments, the loss and storage moduli, associated with viscosity and elasticity, respectively, are presented. Above a transition temperature, not only does the viscosity decrease but also the normal force and the elastic modulus tend to vanish, suggesting that the non-Newtonian behavior is also strongly related to the temperature. Furthermore, the departure from linearity of the logarithm of zero-shear viscosity versus the inverse of the temperature appears to correlate with the transition from non-Newtonian to Newtonian behavior.

1. INTRODUCTION

The variation of the viscosity with the temperature is one of the most important parameters in the oil industry. This variation is related to structural changes, such as asphaltene deposition and wax aggregates, formed during cooling.[1,2]

Intermolecular interactions and structure are responsible for the origin of viscosity and go from simply the area that obstructs the kinematics (for diluted gases) to complex molecular and intermolecular forces that depend upon the chemical characteristics of the material.[3] The simplest definition for the viscosity of liquids is "the resistance to flow",[4] and then it cannot be determined if "flow" is not presented, which contradicts the dilute gas limit at which the viscosity does not vanish. Even more, to have "flow", a velocity field must be implicit, with the associated stress field. The Newton law for viscosity is given by the expression

$$\tau = \eta\dot{\gamma} \tag{1}$$

where η is the viscosity, τ is the shear stress, and $\dot{\gamma}$ is the shear rate.[4] This definition of the viscosity is a simplification that considers a special case of flow: the flow between parallel plates (shear flow). However, the complete description of viscous behavior requires (1) the full stress tensor, which represents the forces in the three-dimensional space, and (2) the velocity gradient tensor, which represents the strain rate in the space. These characteristics make the viscosity a "material function", meaning that the property cannot be described as scalar, because it is not a "state function". The isotropic pressure of a fluid in static equilibrium, which is an example of a state function, can be described in terms of density and temperature but not the viscosity. To simplify this problem, under control conditions, a simple shear geometry, such as parallel plates, where the axial force is proportional to the shear stress and the angular velocity is proportional to the shear rate, may allow for the development of simple shear flow. Therefore, the system reduces to the Newton law for viscosity. When the fluid is non-Newtonian, the viscosity depends upon the shear rate and the presence of normal stresses may also be observed. Then, the equation of the viscosity is written as $\eta = \tau/\dot{\gamma}$, where η is the (shear) viscosity in steady simple shear flow. It is important to mention that to have a reproducible measurement of the viscosity, steady-state conditions should be reached to maintain a constant velocity gradient. In the parallel plates geometry, the first normal stress difference N_1, which is related to elasticity, can be measured by the force that the fluid exerts on the surface of the plates. The presence of elasticity, however, could drastically change the flow, even in an extremely simple context.

Figure 1 denotes the flow generated by a rotating disk in the bottom of a tank. For a Newtonian fluid (pure glycerol), the liquid is accelerated at the top of the disk and the liquid is projected to the walls of the container, generating a downward vortex. On the other hand, a non-Newtonian viscoelastic fluid, consisting of a polymeric aqueous solution, exhibits the opposite behavior. In this case, the elasticity of the material promotes the presence of normal forces, which are larger at the center of the disk, where the largest rate of shearing is located,

Special Issue: 15th International Conference on Petroleum Phase Behavior and Fouling

Received: September 25, 2014
Revised: December 9, 2014
Published: December 26, 2014

DOI: 10.1021/ef502171d
Energy Fuels 2015, 29, 2883−2889

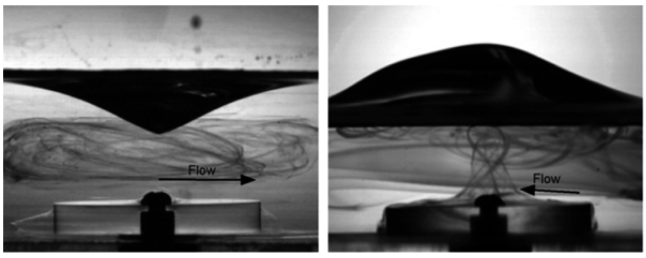

Figure 1. Rotational flow around a disk in a (left) Newtonian fluid and (right) non-Newtonian fluid.

generating an upward vortex. To visualize the flow streamlines, some of the liquid is dyed with vegetable colorant and injected to the setup of Figure 1, clearly denoting the different flow behavior patterns between a Newtonian and non-Newtonian fluid of about similar, otherwise, state properties.

Despite that the non-Newtonian and viscoelastic behavior of heavy oils is well-known,[1,5−11] experimental and modeling efforts are not as extensive as for Newtonian fluids. The main purpose of this work is to present the contribution of the elasticity to the non-Newtonian fluid behavior of heavy oils and its relation with the temperature and to attempt to determine a pragmatic temperature point of transition from a viscoelastic fluid behavior to a Newtonian fluid behavior.

2. EXPERIMENTAL SECTION

2.1. Materials and Oil Conditioning. Five stabilized Mexican heavy oils from different regions of the country with an American Petroleum Institute (API) gravity of around 12° but different chemical structures and compositions were analyzed.[12] The oils were degassed and centrifuged at 2200 rpm, 45 °C, and up to 18 h, until most of the water separated. The water content was estimated by Karl Fischer and reported in Table 1. The wax appearance temperature (WAT) is also reported in Table 1; it was obtained with the use of a cross-polar microscope (accurate to ±1 °C). In addition, a standard silicon oil provided by Aldrich (378402-1L) with a nominal viscosity of 10 000 mPa s at 25 °C is included in the study to present a fluid with a simple rheology and compare such behavior to that exhibited by heavy oils. In Table 1, the main properties of the oils are presented.

2.2. Rheological Analysis. The rheological measurements are performed with an ARES G2 strain-controlled rheometer with temperature control. Parallel plates (40 mm), with a 1 mm gap, are selected to perform the shear flow and oscillatory experiments. For the shear flow, the measurements are obtained in steady-state conditions with the criteria that the viscosity value must remain constant (error < 1%) for every point. The normal force is measured by means of a force transducer located at the upper plate; for this geometry, the lowest reliable value of the first normal stress difference is 20 Pa. Even though the rheometer is able to reach a shear rate up to 1200 s^{-1}, the condition of homogeneous flow is not satisfied at high shear rates and most measurements were stopped at 100 s^{-1}. In general, for viscous materials, the inertial and elastic effects may result in the fluid coming out of the measuring geometry space or starting to slip at the contact surface.[13] The same criterion is used for the oscillatory measurements with the addition of staying within the viscoelastic linear regime. A Stabinger viscometer (Anton-Paar) is used as a reference device to calculate the density, the API gravity, and the viscosity of the oils. In addition to the viscosity, the Stabinger viscometer also reports the shear rate for the measured points; this point is referenced to the flow curves of the Ares G2 rheometer to ensure full agreement between both techniques. In some cases, boiling temperatures below 100 °C are observed when density and viscosity abruptly drop with an increment in the temperature during the Stabinger viscometer measurements.

3. RESULTS AND DISCUSSION

3.1. Temperature Dependence. In Table 1, it can be observed that API is quite similar among the studied oils, whereas the viscosity changes almost 5 times and the boiling at atmospheric conditions may vary more than 30 °C. It is clear that, in these cases, neither the molecular weight nor the API gravity give a direct correlation to viscosity. To study this issue further, rheological characterization and viscosity analysis are presented. A thermorheological simple fluid allows for the use of the superposition of the effects of the time and temperature, which we can associate just to the increment in kinetic energy. In simple fluids, other mechanisms, such as phase change, structural rearrangement, and segregation, among other phenomena, are not present. As mentioned before, to measure the shear viscosity, a simple velocity gradient is required; in the region of low shear rates, the fluids tend to behave as Newtonian, and this defines the "zero-shear viscosity".

The most commonly used model to correlate the temperature dependence of the viscosity of a fluid is the Arrhenius equation, $\eta(T) = A \exp[E_a/(RT)]$, in which η is the viscosity, T is the absolute temperature, A is a material constant, E_a is the fluid-dependent activation energy, and R is the universal gas constant. This model, however, has been shown not to be appropriate for some crude oils.[11,14,15] Other models may provide a more accurate representation, such as the Williams, Landel, and Ferry (WLF) equation[16,17]

$$\log\left(\frac{\eta T_r \rho_r}{\eta_r T \rho}\right) = \log a_T = -\frac{C_1(T - T_r)}{[C_2 + (T - T_r)]} \quad (2)$$

where η, T, and ρ are, the viscosity, the absolute temperature, and the density, respectively. The index "r" refers to a reference state, and C_1 and C_2 are fitting constants. The change in the product of the temperature times density is small and, thus, often ignored ($T_r \rho_r/T\rho \approx 1$). Typically, the reference state is predetermined as the glass transition temperature;[11,14,18] however, after Dobson,[18,19] in this work, the reference temperature was taken as an adjustable parameter.

The WLF and Arrhenius models where fitted to the zero-shear viscosity by means of a nonlinear least-squares regression. The WLF constants C_1, C_2, and T_r are presented in Table 2. In Figure 2, the zero-shear viscosity dependence with the temperature for silicon oil is presented, showing a good

Table 1. Properties of the Studied Fluids

oil	API gravity (deg)	M_w (g/mol)	$T_{boilling}$ (°C)	WAT (°C)	viscosity at 20 °C (Pa s)	water content (wt %)
1	12.3	427.3	>100	36.7	50.1	0.10
2	12.2	418.5	>100	18.8	44.3	0.07
3	12.3	408.4	∼80	42.7	29.8	1.41
4	12.1	409.1	∼80	−10	20.0	0.20
5	12.4	398.1	∼70	−10	13.6	0.12
silicon	28.8		>250		10.9	

DOI: 10.1021/ef502171d
Energy Fuels 2015, 29, 2883−2889

Table 2. Parameters of the WLF Model and Transition Temperature (T_0)

oil	C_1	C_2 (K)	T_r (K)	correlation r^2	T_0 (K)
1	10.005	137.868	330.65	1.0000	307.59
2	9.972	138.102	330.47	1.0000	307.71
3	12.139	160.999	328.33	0.9999	308.51
4	10.710	150.655	323.67	1.0000	310.14
5	10.400	147.296	322.20	1.0000	310.53
silicon	12.083	181.677	319.23	0.9999	313.49

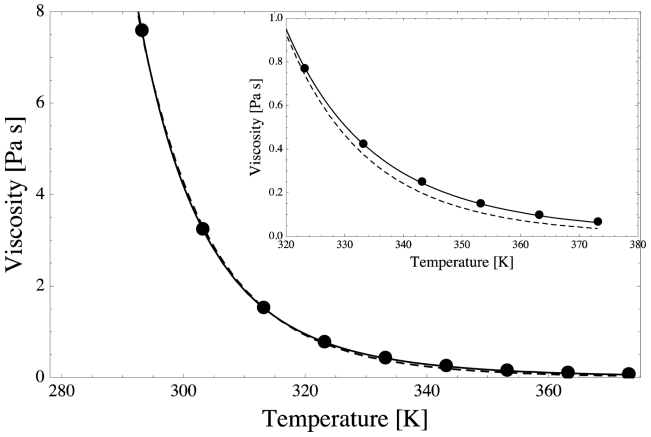

Figure 2. Viscosity of silicon oil as a function of the temperature. The symbols correspond to the experimental points, and the curves correspond to the (—) WLF model and (- - -) Arrhenius model. The inset shows the model departure in the low-viscosity region.

correlation to the WLF equation. A comparison is also made with the Arrhenius equation, which does not fit the data well at high temperatures. In Figure 3, the zero-shear viscosity dependence with the temperature for the five oils along with the WLF model fits are presented.

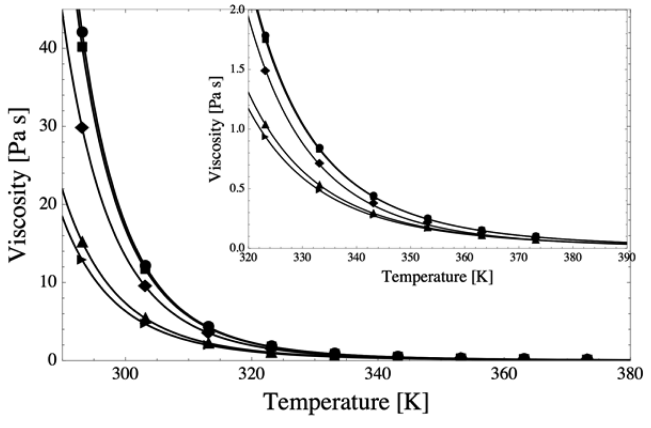

Figure 3. Zero-shear viscosity as a function of the temperature for the five heavy oils. The solid curves represent the WLF model fit, and the symbols represent the experimental points: (●) oil 1, (■) oil 2, (◆) oil 3, (▲) oil 4, and (▶) oil 5.

According to the correlation coefficients (r^2), in Table 2, the WLF model delivers a good description of the zero-shear viscosity as a function of the temperature for all of the studied fluids. If the data are plotted in the form of $\log[\eta]$ against $1/T$, a departure from linearity is found (Figure 4), which indicates that the fluid is not "thermorheological simple". This departure

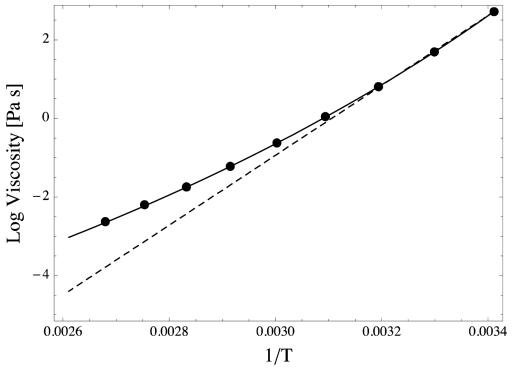

Figure 4. Identification of the transition temperature for oil 4 denoted by the intersection between the (—) WLF model and (- - -) Arrhenius linear model.

from linearity may be correlated to a transition temperature from viscoelastic to viscous or from shear thinning to Newtonian behavior. This departure may also indicate some sort of molecular structuring or ordering under shear, as observed by molecular simulations.[20−22]

A reasonable approximation for the transition temperature appears to be the point of departure from a linear Arrhenius model, as in Figure 4. This transition may be approximated by the intersection between WLF and Arrhenius models, after which the model differences become negligible. The estimated transition temperatures T_0 for the five oils studied in this work are also reported in Table 2.

3.2. Simple Shear Flow. In Figures 5 and 6, the shear flow viscosity and first normal stress difference as a function of the

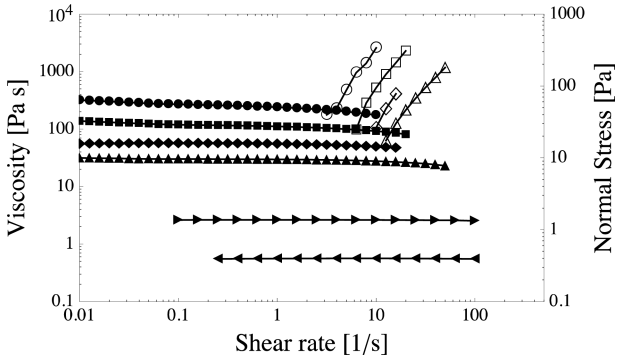

Figure 5. (Filled symbols) Shear viscosity and (open symbols) first normal stress difference at steady state for oil 3 as a function of the temperature: (● and ○) T = 5 °C, (■ and □) T = 10 °C, (◆ and ◇) T = 15 °C, (▲ and △) T = 20 °C, (▶) T = 40 °C, and (◀) T = 60 °C.

temperature, for the oils 3 and 4, are presented. In both cases, the viscosity and shear-thinning behavior decrease as the temperature increases. At 40 °C, the normal stress cannot be any further reliably measured, which indicates that the fluid mainly behaves as a viscous material. That is, as long as no shear thinning is observed, the fluid behaves as Newtonian fluid, and this appears to be consistent with the suggested transition temperature reported in Table 2.

Because of the high viscosity of oil 3, it is not possible to reach higher shear rates for temperatures among 5 and 20 °C, whereas for 40 and 60 °C, the viscosity remains almost

DOI: 10.1021/ef502171d
Energy Fuels 2015, 29, 2883−2889

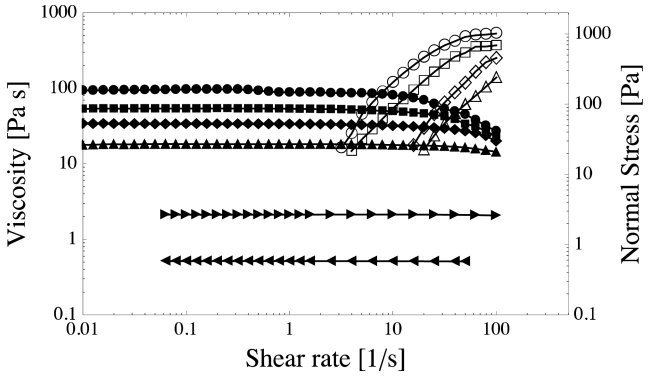

Figure 6. (Filled symbols) Shear viscosity and (open symbols) first normal stress difference at steady state for oil 4 as a function of the temperature: (● and ○) T = 5 °C, (■ and □) T = 10 °C, (◆ and ◇) T = 15 °C, (▲ and △) T = 20 °C, (▶) T = 40 °C, and (◀) T = 60 °C.

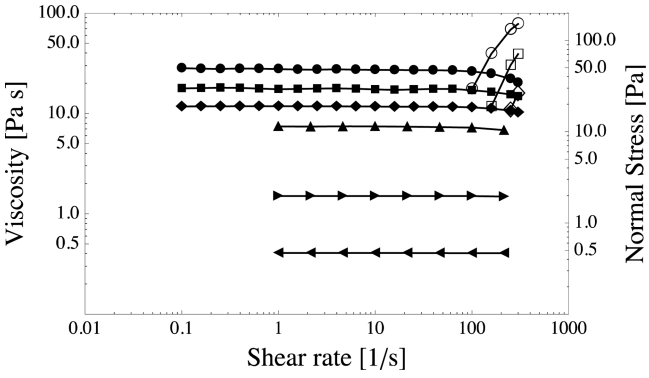

Figure 7. (Filled symbols) Shear viscosity and (open symbols) first normal stress difference at steady state for silicon oil as a function of the temperature: (● and ○) T = 5 °C, (■ and □) T = 10 °C, (◆ and ◇) T = 15 °C, (▲) T = 20 °C, (▶) T = 40 °C, and (◀) T = 60 °C.

constant. The normal force increases as the shear rate increases and decreases with the increment of the temperature.

Oil 4 has a lower viscosity than oil 3; then higher shear rates can be reached; and a wider region of shear thinning can be measured. It can be seen that, for 5 °C, the oil exhibits shear thinning, and as long as the temperature increases, the shear thinning moves to higher shear rates, until it vanishes for temperatures near 40 °C, becoming the Newtonian fluid for the measured shear rate studied in this work. The normal stress has a similar behavior, with the particularity that, at 5 °C, the normal stress reaches a plateau at a high shear rate, as predicted by some authors.[23] In both cases, the change from viscoelastic to Newtonian appears to correlate reasonably well with the "transition temperature", as determined in the previous section. It is worth mentioning that the viscosity drops 3 orders of magnitude with the increment of the temperature of around 50 °C for both oils; the other oils present a similar behavior. It should also be pointed out that, while the non-Newtonian behavior shown by oil 3 is below the WAT, this is not the case for oil 4, which indicates that non-Newtonian behavior is not necessarily related to the crystallization of paraffinic wax. In Table 3, the saturates, aromatics, resins, and asphaltenes

Table 3. SARA Analysis of Oils

oil	saturates (wt %)	aromatics (wt %)	resins (wt %)	asphaltenes (wt %)
1	30.4	25.1	23.0	19.1
2	26.4	30.6	27.3	18.5
3	24.3	28.0	30.7	14.5
4	21.4	37.2	28.5	12.2
5	22.4	34.7	28.9	12.0

(SARA) analysis of the oils is presented. A relation between viscosity and asphaltene content is evident; as the content of asphaltenes increases, the viscosity also increases. This relation will be further studied in forthcoming works.

In Figure 7, the shear flow viscosity and first normal stress difference as a function of the temperature for silicon oil are presented. Viscoelastic behavior appears at a high shear rate with smaller values in normal stress than oils 3 and 4. This means that silicon oil preferably behaves as a Newtonian fluid.

3.3. Small-Amplitude Oscillatory Flow. In contrast to shear flow measurements, small-amplitude oscillatory experiments preserve the structure of the fluid; i.e., the fluid does not undergo a shear-flow-induced structural rearrangement.[4,13,24] Some fluids present viscoelasticity, which clearly implies a dual behavior, where the material exhibits a mix of liquid and solid-like characteristics. In the oscillatory experiments, a stress is applied and the response of the material is measured. From this information, the loss and storage moduli are determined. The first corresponds to the viscous part of the material considered as the capacity to dissipate the applied energy, while the storage modulus is related to the elastic part of the material. The viscoelasticity depends upon the deformation rate; therefore, at a low deformation rate, the materials behave like a liquid, and at a high deformation rate, the materials behave like a solid. To illustrate this idea, in Figure 8, the loss G'' and storage G'

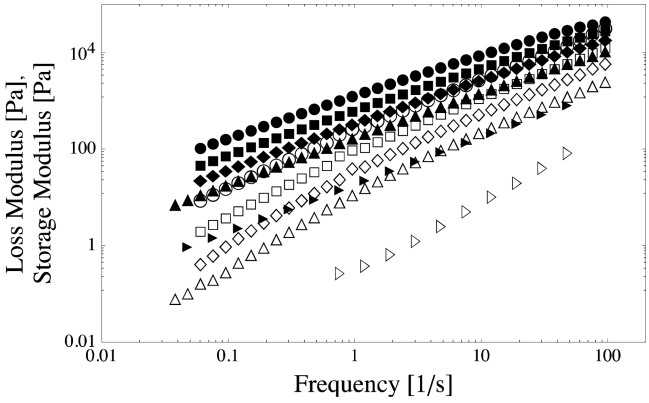

Figure 8. (Filled symbols) Loss and (open symbols) storage moduli for oil 3 at different temperatures: (● and ○) T = 5 °C, (■ and □) T = 10 °C, (◆ and ◇) T = 15 °C, (▲ and △) T = 20 °C, and (▶ and ▷) T = 40 °C.

moduli of oil 3 are depicted as a function of frequency at different temperatures. The magnitude of the loss modulus is higher than the magnitude of the storage modulus in all of the cases. As the temperature increases, the magnitude of both moduli decreases too. In Figure 9, the loss G'' and storage G' moduli as a function of the frequency at different temperatures for silicon oil are presented. It can be observed that G'' is much bigger than G', with the latter appearing at high shear rates. This agrees with the rheology observed in Figure 7.

To quantify the viscoelasticy of the material, the angle

DOI: 10.1021/ef502171d
Energy Fuels 2015, 29, 2883−2889

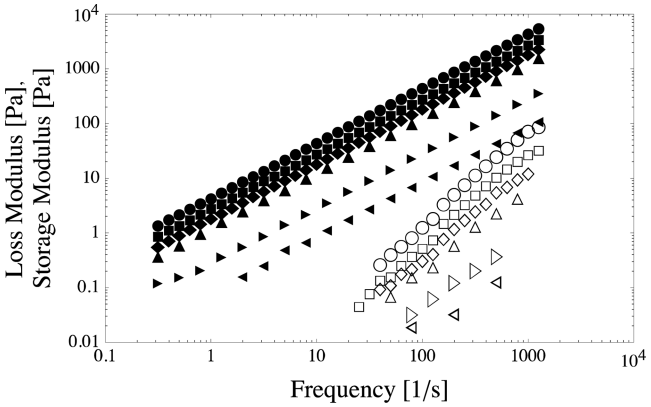

Figure 9. (Filled symbols) Loss and (open symbols) storage moduli for silicon oil at different temperatures: (● and ○) T = 5 °C, (■ and □) T = 10 °C, (◆ and ◇) T = 15 °C, (▲ and △) T = 20 °C, (▶ and ▷) T = 40 °C, and (◀ and ◁) T = 60 °C.

$$\delta = \arctan\left(\frac{G''}{G'}\right) \tag{2}$$

is defined.[4] The angle varies from 0 to 90 grads, which corresponds from pure elastic to pure viscous behavior. In Figure 10, the angle δ as a function of the frequency at different

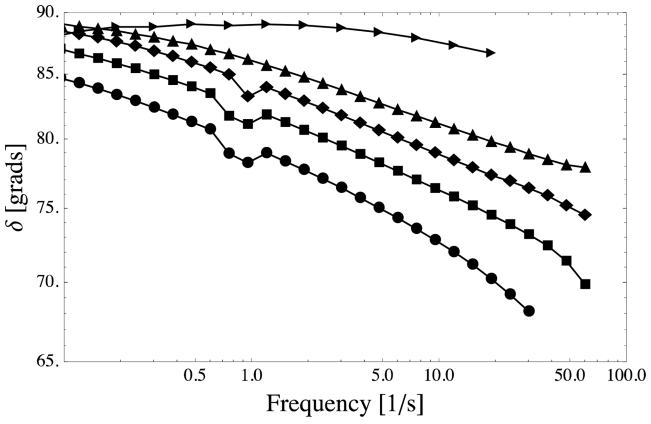

Figure 10. Angle δ as a function of the frequency for oil 3 at different temperatures: (●) T = 5 °C, (■) T = 10 °C, (◆) T = 15 °C, (▲) T = 20 °C, and (▶) T = 40 °C.

temperatures for oil 3 is presented. As the frequency increases, the angle decreases, which implies that the elastic modulus contribution increases. With the increment of the temperature, the angle increases; therefore, the viscous modulus dominates and the non-Newtonian effect vanishes. It is clearly observed that, at low frequency, for 40 °C, the angle has a value close to 90 grads.

In Figure 11, the angle δ as a function of the frequency at different temperatures for silicon oil is presented. It is very clear that the viscous effect governs over elastic behavior, because the angle δ is practically 90 grads for all temperatures. A very slow reduction of the angle can be observed for high frequencies.

In Figure 12, the angle δ dependence with the temperature for the five oils is presented. The angles increase as the temperature increases, which mean that the elastic part of the oil vanishes with the temperature. Oil 1, which exhibits the highest zero-shear viscosity in Table 1, reaches the lowest value of the angle δ; oils 1 and 2 are the most viscoelastic oils. As

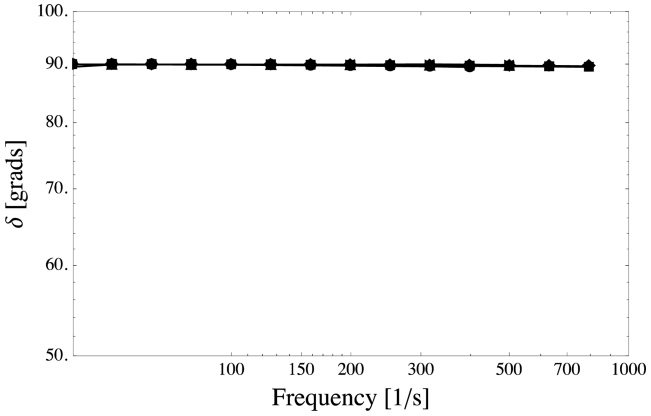

Figure 11. Angle δ as a function of the frequency for silicon oil at different temperatures: (●) T = 5 °C, (■) T = 10 °C, (◆) T = 15 °C, (▲) T = 20 °C, and (▶) T = 40 °C.

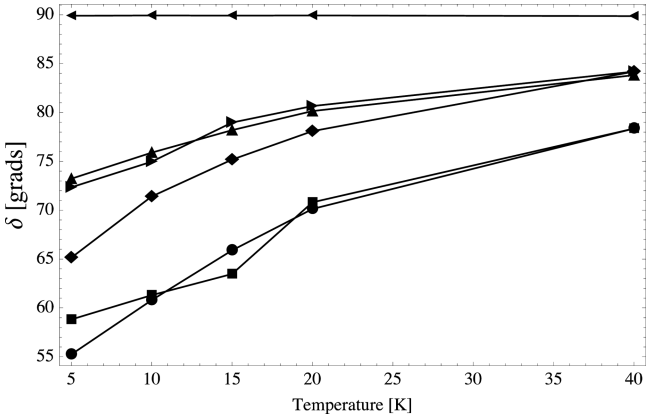

Figure 12. Angle δ as a function of the temperature for the five oils at a constant frequency (50 s^{-1}) at different temperatures: (•) oil 1, (■) oil 2, (◆) oil 3, (▲) oil 4, (▶) oil 5, and (◀) silicon oil.

mentioned before, silicon oil is not a viscoelastic fluid and is practically a pure viscous fluid, as clearly demonstrated in Figures 11 and 12.

In the oscillatory experiments, an equivalent of the shear flow viscosity is defined as[16]

$$\eta^* = \frac{\sqrt{G'^2 + G''^2}}{\omega} \tag{3}$$

where η^* is called the simple shear complex viscosity and ω is the oscillation frequency. When both viscosities have the same value, the fluid is rheologically simple and follows the Corx–Merz rule;[24] otherwise, the fluid tends to change its structure under flow, creating or destroying the structure, and a separation between viscosities is observed.

Figures 13, 14, and 15 show a comparison of both viscosities for oil 3, oil 4, and silicon oil, respectively, at different temperatures. Below the transition temperature, the fluids develop a separation between both viscosities, which confirms the suggested criterion for introducing a transition temperature; the viscoelastic behavior of silicon oil is observed only at high shear rates. For temperatures above the transition temperature, the complex and shear viscosities closely match for all cases. As long as the complex viscosity has a smaller magnitude than the shear viscosity, the shear flow induces structure formation,

DOI: 10.1021/ef502171d
Energy Fuels 2015, 29, 2883–2889

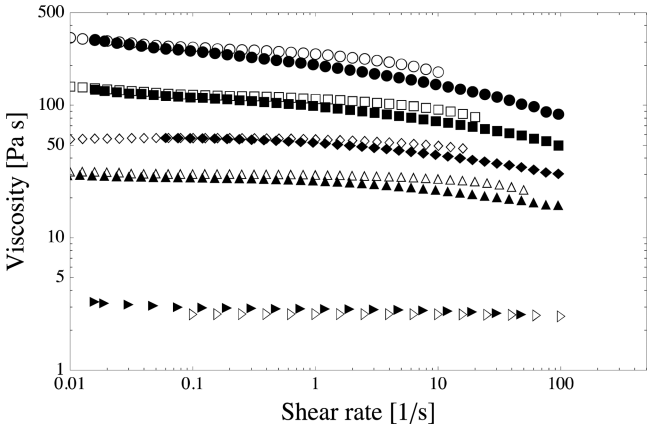

Figure 13. (Filled symbols) Complex viscosity and (open symbols) shear viscosity at steady state for oil 3 as a function of the temperature: (● and ○) T = 5 °C, (■ and □) T = 10 °C, (◆ and ◇) T = 15 °C, (▲ and △) T = 20 °C, and (▶ and ▷) T = 40 °C.

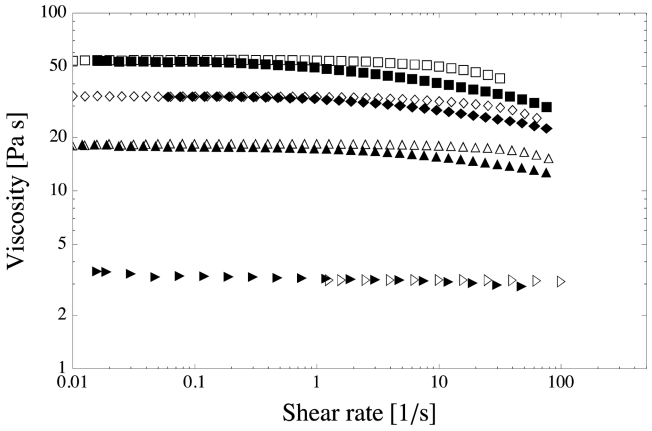

Figure 14. (Filled symbols) Complex viscosity and (open symbols) shear viscosity at steady state for oil 4 as a function of the temperature: (● and ○) T = 5 °C, (■ and □) T = 10 °C, (◆ and ◇) T = 15 °C, (▲ and △) T = 20 °C, and (▶ and ▷) T = 40 °C.

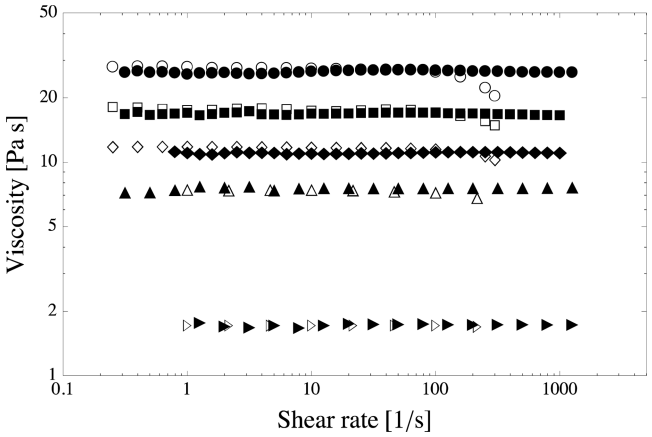

Figure 15. (Filled symbols) Complex viscosity and (open symbols) shear viscosity at steady state for silicon oil as a function of the temperature: (● and ○) T = 5 °C, (■ and □) T = 10 °C, (◆ and ◇) T = 15 °C, (▲ and △) T = 20 °C, and (▶ and ▷) T = 40 °C.

which may indicate the aggregation of some components of the oils, such as asphaltenes or paraffin waxes.

4. CONCLUSION

The rheological properties of heavy oils are strongly related to the temperature. Behavior changes appear to be identified by a change of slope in the plot of log[viscosity] versus the inverse of the temperature. A fluid, such as the silicon oil presented here, whose structure does not undergo a significant change, does not show this behavior. From the measured viscosity, it is possible to identify a "transition temperature", which is associated with the transition from Newtonian to non-Newtonian behavior as the temperature is lowered and the fluid structure becomes stronger. Although the non-Newtonian behavior may be enhanced by the crystallization of paraffin wax, a fluid structural change rather than phase transition correlates the phenomenon. This observation is corroborated by the vanishing of the shear thinning effects and the decrease of the normal stress with the increment of the temperature. The small-amplitude oscillatory experiments confirm the previous conclusion by the angle δ determined from the ratio between the loss and storage moduli. Finally, an indication of the change in the internal structure of the oils is observed by the comparison of the shear and complex viscosities, clearly indicating the flow complexity of heavy oils.

■ AUTHOR INFORMATION

Corresponding Author

*E-mail: seqc@unam.mx.

Notes

The authors declare no competing financial interest.

■ ACKNOWLEDGMENTS

Support for this work has been provided by the "Fondo Sectorial SENER−CONACY−Hidrocarburos" (Grant 160015). The authors acknowledge the support of personnel from PEMEX in the realization of our research program and Prof. Roberto Zenit for his help in the acquisition of the pictures in Figure1.

■ REFERENCES

(1) Roenningsen, H. P.; Bjoerndal, B.; Baltzer Hansen, A.; Batsberg Pedersen, W. Wax precipitation from North Sea crude oils: 1. Crystallization and dissolution temperatures, and Newtonian and non-Newtonian flow properties. *Energy Fuels* **1991**, *5* (6), 895−908.

(2) Cimino, R.; Correra, S.; Del Bianco, A.; Lockhart, T. Solubility and phase behavior of asphaltenes in hydrocarbon media. In *Asphaltenes*; Sheu, E., Mullins, O., Eds.; Springer: New York, 1995; pp 97−130.

(3) Lautrup, B. *Physics of Continuous Matter: Exotic and Everyday Phenomena in the Macroscopic World*; Institute of Physics Publishing: Bristol, U.K., 2005.

(4) Morrison, F. A. *Understanding Rheology*; Oxford University Press: New York, 2001.

(5) Quiñones-Cisneros, S. E.; Schmidt, K. A. G.; Creek, J.; Deiters, U. K. Friction theory modeling of the non-Newtonian viscosity of crude oils. *Energy Fuels* **2008**, *22* (2), 799−804.

(6) Ramírez-González, P. V.; Aguayo, J. P.; Quiñones-Cisneros, S. E.; Deiters, U. K. Non-Newtonian viscosity modeling of crude oils—Comparison among models. *Int. J. Thermophys.* **2009**, *30* (4), 1089−1105.

(7) Dante, R. C.; Geffroy, E.; Chávez, A. E. Adam−Gibbs theory applied to a unifying rheological model of crude oil and alkanes. *Energy Fuels* **2007**, *21*, 903−911.

(8) Pedersen, K. S.; Rønningsen, H. P. Effect of precipitated wax on viscosity—A model for predicting non-Newtonian viscosity of crude oils. *Energy Fuels* **2000**, *14*, 43−51.

DOI: 10.1021/ef502171d
Energy Fuels 2015, 29, 2883−2889

(9) Pedersen, K. S.; Fredenslund, A.; Thomasson, P. *Properties of Oils and Natural Gases*; Gulf Publishing Company: Houston, TX, 1989; p 182.
(10) Li, H.; Zhang, J. A generalized model for predicting non-Newtonian viscosity of waxy crudes as a function of temperature and precipitated wax. *Fuel* **2003**, *82*, 1387−1397.
(11) Abivin, P.; Taylor, S. D.; Freed, D. Thermal behavior and viscoelasticity of heavy oils. *Energy Fuels* **2012**, *26* (6), 3448−3461.
(12) Soto, E.; Ramírez-González, P. V.; Quiñones-Cisneros, S. E. Rheological behavior of basic oils and blends; from 8 to 40 API gravity. *Proceedings of the 15th International Conference on Petroleum Phase Behavior and Fouling (Petrophase XV)*; Galveston, TX, June 8−12, 2014.
(13) Barnes, H. A. *A Handbook of Elementary Rheology*; Institute of Non-Newtonian Fluid Mechanics, University of Wales: Aberyswyth, U.K., 2000.
(14) Lesueur, D.; Gerard, J. F.; Claudy, P.; Letoffe, J. M.; Planche, J. P.; Martin, D. A structure-related model to describe asphalt linear viscoelasticity. *J. Rheol.* **1996**, *40* (5), 813−836.
(15) Dymond, J. H.; Øye, H. A. Viscosity of selected liquid *n*-alkanes. *J. Phys. Chem. Ref. Data* **1994**, *23* (1), 41−53.
(16) Macosko, C. W. *Rheology: Principles, Measurements, and Applications*; Wiley-VCH: Poughkeepsie, NY, 1994.
(17) Ngai, K.; Plazek, D. Temperature dependences of the viscoelastic response of polymer systems. In *Physical Properties of Polymers Handbook*; Mark, J., Ed.; Springer: New York, 2007; pp 455−478.
(18) Lesueur, D. The colloidal structure of bitumen: Consequences on the rheology and on the mechanisms of bitumen modification. *Adv. Colloid Interface Sci.* **2009**, *145* (1−2), 42−82.
(19) Dobson, G. R. *The Dynamic Mechanical Properties of Bitumen*; British Petroleum Company: London, U.K., 1969.
(20) Ramírez-González, P. V. Propiedades reológicas e interfaciales de fluidos complejos mediante simulación molecular. Ph.D. Thesis, Universidad Nacional Autónoma de México, Mexico City, Mexico, 2013.
(21) Kröger, M.; Loose, W.; Hess, S. Rheology and structural changes of polymer melts via nonequilibrium molecular dynamics. *J. Rheol.* **1993**, *37* (6), 1057−1079.
(22) Delhommelle, J.; Petravic, J.; Evans, D. J. Non-Newtonian behavior in simple fluids. *J. Chem. Phys.* **2004**, *120* (13), 6117−6123.
(23) Bautista, F.; de Santos, J. M.; Puig, J. E.; Manero, O. Understanding thixotropic and antithixotropic behavior of viscoelastic micellar solutions and liquid crystalline dispersions. I. The model. *J. Non-Newtonian Fluid Mech.* **1999**, *80* (2−3), 93−113.
(24) Manero, O.; Bautista, F.; Soltero, J. F. A.; Puig, J. E. Dynamics of worm-like micelles: The Cox−Merz rule. *J. Non-Newtonian Fluid Mech.* **2002**, *106*, 1−15.

DOI: 10.1021/ef502171d
Energy Fuels 2015, 29, 2883−2889